ACS APPLIED MATERIALS & INTERFACES

Research Article

www.acsami.org

Well-Ordered Nanoporous ABA Copolymer Thin Films via Solvent Vapor Annealing, Homopolymer Blending, and Selective Etching of ABAC Tetrablock Terpolymers

Elizabeth A. Jackson,[§] Youngmin Lee,[§] Madalyn R. Radlauer, and Marc A. Hillmyer*

Department of Chemistry, University of Minnesota, Minneapolis, Minnesota 55455-0431, United States

Supporting Information

ABSTRACT: Solvent vapor annealing treatments are used to control the orientation of nanostructures produced in thin films of a poly(styrene)-*block*-poly(isoprene)-*block*-poly(styrene)-*block*-poly((±)-lactide) (PS−PI−PS−PLA) and its blends with PLA homopolymer. The PS−PI−PS−PLA tetrablock terpolymer, previously determined to adopt a core(PLA)−shell(PS) cylindrical morphology in the bulk, gave perpendicular alignment of PLA cylinders over a limited range of thicknesses using a mixed solvent environment of tetrahydrofuran and acetone. On the other hand, perpendicular alignment was achieved regardless of film thickness by inclusion of 5 wt % homopolymer PLA in the PS−PI−PS−PLA tetrablock. Tapping mode atomic force microscopy (AFM) was used to visualize film surface morphologies. Subsequent reactive ion etching (RIE) and basic hydrolysis of PLA produced 15 nm pores in a PS−PI−PS triblock thin film matrix. Nanoporosity was confirmed by scanning electron microscopy (SEM) images and the vertical continuity of pores was confirmed by cross-sectional SEM analysis.

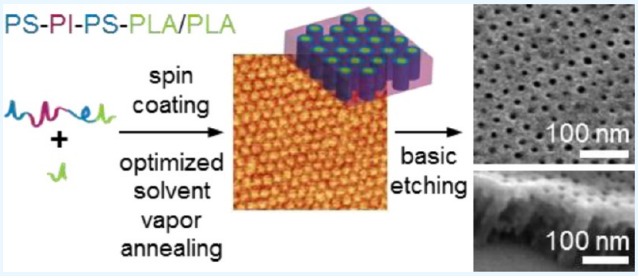

KEYWORDS: *tetrablock terpolymers, solvent vapor annealing, homopolymer blending, selective etching, nanoporous thin films, perpendicularly oriented cylinders*

INTRODUCTION

Ordered block polymer thin films have received much attention as enabling platforms for various nanotechnology applications.[1−6] For example, self-assembled block polymer thin films have led to improvements in the fabrication of high-density information storage media,[7−10] nanoporous membranes,[11−15] nano-objects,[16] photonic band gap materials,[17] semiconductors,[18,19] magnetic storage materials,[20] and nanomaterials.[21,22] Many of these applications rely on thin films containing cylindrical or lamellar morphologies.[5,6] For membranes and other templating applications, it is often desirable for the films to contain sacrificial (i.e., etchable) domains that can be selectively and completely removed to produce pores that fully traverse the entire film thickness.

PLA has found great utility as a sacrificial block in many block polymer systems in bulk and thin films because of the efficiency of PLA hydrolysis.[14,23−28] Because of the rather large interaction parameter between PLA and less polar polymers, such as PI,[29] ultrasmall domains are accessible (<10 nm).[30] Multiple reports have shown that it is possible to obtain perpendicular orientation of PLA domains (at the surface of the film) through spin coating, as demonstrated for PS−PLA,[24,28] PS−PI−PLA,[26,27,31] and PS−PI−PS−PLA.[32] Yet spin coating alone can be undesirable for membrane and templating applications since it often does not allow for morphology organization throughout the entire film.

In this Research Article, the thin film alignment of a poly(styrene)-*block*-poly(isoprene)-*block*-poly(styrene)-*block*-poly((±)-lactide) (PS−PI−PS−PLA) tetrablock terpolymer is examined. The block polymer used for this study contains a volume fraction of PLA (f_{PLA}) of 0.21 and adopts a core(PLA)−shell(PS) hexagonally packed cylindrical morphology in the bulk state.[32] ABAC structured block polymers have been shown to exhibit interesting phase behavior in the bulk but their thin film behavior has not received much attention.[33−37] In our previous work on PS−PI−PS−PLA, we observed that the physically cross-linked PS−PI−PS blocks produced an inherent mechanical toughness after selective etching of the PLA domains.[32] The combination of the rigid PS blocks and the rubbery PI block results in a robust film.[31] These thin films, however, did not exhibit long-range order, motivating further study. Both toughness and long-range order are essential characteristics of nanoporous films for high performance filtration membranes, pattern transfer masks, and other applications that require mechanical integrity in the self-assembled film structure.

Many strategies that have been employed to control block polymer structure in thin films include thermal annealing,[11]

Received: September 18, 2015
Accepted: November 23, 2015
Published: December 7, 2015

DOI: 10.1021/acsami.5b08856
ACS Appl. Mater. Interfaces 2015, 7, 27331−27339

solvent vapor annealing,[38] electrical field alignment,[39] and controlled solvent evaporation.[22] Simulation and experiments have shown that the film morphology of cylinder- and lamellae-forming diblock copolymers is dependent on the relative interfacial interactions of the blocks and the commensurability between the film thickness and block polymer domain spacing.[25] To control the orientation of domains, the interfacial preference of the constituent blocks must be controlled during annealing so that it is energetically favorable for all blocks in the sample to be at the interfaces. Otherwise the preferential interaction of one constituent with a surface can lead to selective enrichment of that block at the substrate−polymer (or air−polymer) interface favoring microdomains parallel to the substrate surface.

Solvent vapor annealing (SVA) is one useful technique that can promote well-ordered perpendicular arrays of AB and ABC block polymers.[1−4,6,25,28,38,40] Unlike thermal annealing, SVA allows faster alignment, better control over interfacial phenomena, and can be accomplished at low temperature.[25,38,41] Degradation of PLA[42,43] at high temperatures can render thermal annealing requiring high temperatures (>200 °C) or long annealing times challenging for PLA-containing block polymers.[44] Because of this, SVA is especially well suited for PLA containing films. Additionally, SVA is a relatively fast technique that can facilitate organization/alignment of domains in block polymers including those with high interaction parameters and high molar masses.[45] Mixed solvent SVA has been employed to more finely tune the surface energy/environment of specific block polymer systems and control morphology.[46−51]

Achieving a balance between interfacial tensions does not guarantee perpendicular orientation.[22] Combined annealing techniques including raster SVA (RSVA),[52] solvothermal annealing,[53] SVA with soft shear (SVA-SS),[54] and RSVA-SS[55] have been utilized to improve orientation. Another technique that has received recent attention involves the incorporation of homopolymer.[56] Such homopolymer/copolymer blends have allowed thickness independent perpendicular cylinder orientation in films for a variety of copolymer systems including PS−PMMA/PMMA,[56] PS−PEO/PEO and PS−PEO/PMMA,[57] and PS−PI−PS/PS and PS−PB−PS/PS.[58−60] The effect is optimized when the molar mass ratio between the homopolymer and corresponding block is about 1.5 at low homopolymer concentrations.[56] Because of the slight mismatch in chain lengths, it is postulated that elongation of homopolymer chains along the center of the long axis of cylindrical domains occurs to accommodate homopolymer chains within the domain.

Herein, we describe SVA and homopolymer blending to control the morphology of ABAC tetrablock terpolymer thin films. PS−PI−PS−PLA thin films were annealed in good solvents for PI, PS, and PLA: toluene, chloroform, and tetrahydrofuran (THF). Then, to further increase the compatibility with polylactide domains, the annealing solvent polarity was increased by using mixtures of THF and acetone. Finally, a homopolymer additive strategy was employed to encourage higher order and enhanced perpendicular orientation of PLA cylinders. By utilizing advanced techniques to guide the alignment of cylinders in the tetrablock polymer/homopolymer blends pre-etching, the fabricated nanoporous films were endowed with the advantageous combination of toughness and long-range order.

METHODS

Polymer Synthesis. The PS−PI−PS−PLA polymer used in this work had a total molar mass of 27 kg mol^{-1} (M_n (PS) = 11 kg mol^{-1}, M_n (PI) = 9 kg mol^{-1}, M_n (PLA) = 7 kg mol^{-1}) and a dispersity, $Đ$, of 1.09. Synthetic details regarding the preparation of this multiblock terpolymer were reported previously.[32] The tetrablock PS−PI−PS−PLA polymer used in this study adopts a hexagonally packed core(PLA)−shell(PS) cylindrical morphology in the bulk. Domain spacing in the bulk, L_0, was 28.6 nm by SAXS. Using a PS volume fraction of 0.40 and a PLA volume fraction of 0.21, a 33.0 nm cylinder center−center distance was estimated from SAXS. In addition, a PS cylinder diameter of 23.5 nm and a PLA cylinder diameter of 13.8 nm were also estimated from SAXS using the equation for cylindrical domains ($f_{polymer} = 2\pi/(\sqrt{3})(R/D)^2$), where R = radius and D = domain spacing.

Homopolymer PLA was prepared by ring-opening transesterification polymerization (ROTEP) of (±)-lactide from benzyl alcohol using Sn(Oct)$_2$ as the catalyst. The measured M_n was 10 kg mol^{-1} and dispersity was 1.08 as determined from size exclusion chromatography (SEC).

Materials. Annealing solvents were dried over activated molecular sieves (3 Å for acetone, 4 Å for THF, toluene, and chloroform) for 48 h prior to solvent annealing to remove water. Solvents were filtered through 0.45 μm Pall PTFE Acrodisc syringe filters before loading in the solvent reservoir. All polymer solutions were filtered through 0.45 μm Pall PTFE Acrodisc syringe filters before spin coating and used within 1 d after preparation. All other reagents were purchased from Sigma-Aldrich and were used as received.

Molecular Characterization. All ^{1}H NMR spectroscopy experiments were performed at 25 °C on a Varian Inova (500 MHz) instrument with polymer solutions in $CDCl_3$. Chemical shifts were determined as δ (ppm) relative to the ^{1}H signals of $CHCl_3$ at 7.27 ppm. Size exclusion chromatography was used to determine the molar mass and dispersity of PLA homopolymer. SEC was performed on a Hewlett-Packard (Agilent Technologies) 1100 series liquid chromatography equipped with a Hewlett-Packard 1047A refractive index detector. Samples were prepared at concentrations between 1−5 mg/mL in $CHCl_3$, and run at 35 °C with $CHCl_3$ as an eluent through three Plgel 5 μm Mixed-C columns in series with an available molar mass range of 400−400 000 g/mol. The molar masses and dispersities were estimated by polystyrene standards purchased from Polymer Laboratories.

Small Angle X-ray Scattering (SAXS). Polymer and solvent were added to aluminum DSC pans with 25%, 50%, or 75% polymer (by mass). The pans were then sealed and the samples were annealed. SAXS data was collected at the Advanced Photon Source (APS) at Argonne National Laboratory in beamline Sector 5-ID-D. The beamline is maintained by the Dow−Northwestern−Dupont Collaborative Access Team (DND-CAT).

Thin Film Preparation. Hexamethyldisilazane (HMDS) modified Si wafers were produced by sonicating wafers in solvents (acetone, then methanol) for 15 min each, rinsing with isopropanol, immersing in a 1:5 (v/v) HMDS:toluene solution for 16 h, rinsing wafers with toluene, and blowing dry with house nitrogen (N_2) gas. Spin coating of the wafers was achieved by preparing 1.0, 1.5, or 2.0 wt % solutions of PS−PI−PS−PLA or of 95/5 PS−PI−PS−PLA/PLA (w/w) polymer blend in chlorobenzene. Chlorobenzene was chosen because of good solubility of the polymer samples and consistent results obtained from spin coating. Spin coating at ambient conditions was performed at 1500, 2000, and 3000 rpm for 60 s to generate a range of film thicknesses between 30 and 100 nm.

Thin Film Solvent Vapor Annealing. Solvent vapor annealing of films was performed immediately after spin coating. The experimental setup for solvent annealing is presented in Figure S1 and is detailed in a previous publication.[27] To remove any atmospheric humidity or solvent vapors, the entire solvent annealing chamber (including the solvent reservoir) was purged with N_2 gas for 30 min before use. Before each experiment, the solvent reservoir was filled with 150 mL of solvent (either toluene, chloroform, THF, or a mixture of THF and

DOI: 10.1021/acsami.5b08856
ACS Appl. Mater. Interfaces 2015, 7, 27331−27339

acetone) and then sealed off from the sample chamber and atmosphere. Spin coated films were then placed inside the sample chamber and purged with N_2 gas for 10 min. After purging, N_2 gas was then redirected to the solvent line and the valve between the solvent reservoir and sample chamber was opened to introduce solvent vapor into the sample chamber.

Films were swollen with solvent vapor by using a constant flow of N_2 gas (3.8 L min^{-1}) through the solvent reservoir. Solvent absorption was observed by changes in film color after a few seconds. Solvent was removed quickly after a set time (2, 5, 10, or 20 min) by closing off the solvent line to the sample chamber (valve C, Figure S1) and quickly purging the sample chamber with clean N_2 gas (valve B, Figure S1). Higher flow rates oversaturated the films with solvent and caused dissolution of polymer from the Si wafer.

Etching and hydrolysis. Surface wetting layers from annealed films were removed by reactive ion etching (RIE) on an STS etcher model 320. Films were exposed to oxygen (O_2) plasma at 30 mTorr with power of 60 W. We determined that a short ~6−8 s RIE was sufficient to remove the surface wetting layer for all films. To hydrolyze the PLA, samples were immersed in a 0.25 M sodium hydroxide solution containing 40/60 (v/v) methanol/water containing 0.1 wt % of sodium dodecyl sulfate for 45 min without stirring. After removal from solution, films were rinsed first with a 40/60 (v/v) methanol/water solution for 10 min and then briefly with water. The samples were dried with N_2 gas.

Thin Film Analysis. Film thickness was measured by a surface and thin film spectroscopic ellipsometer VASE from J. A. Wollam Co., Inc. Tapping mode atomic force microscopy (AFM) was performed on an Agilent 5500 environmental scanning probe microscope. Scanning electron microscopy (SEM) imaging was performed on a Hitachi S-900 field emission gun scanning electron microscope (FE-SEM). For best resolution and least sample charging, SEM analysis was performed at 2 kV on films coated with 2−3 nm of Pt. For cross-sectional SEM, PLA etched films were immersed in liquid N_2 for 1−2 min before fracturing in the liquid N_2 bath. Prior to SEM, samples were coated for 13 min at a coating rate of 0.2 nm Pt/min with a VCR high resolution indirect ion-beam sputter coater.

For the observation of the bottom surface, the top surface of the polymer film was covered with epoxy resin (EpoFix resin and hardener from Struenrs) and cured for 24 h. The polymer film was then detached from the Si wafer substrate in liquid N_2 to expose the bottom side of the etched film.

RESULTS AND DISCUSSION

Thin films of core(PLA)−shell(PS) cylinder-forming PS−PI−PS−PLA tetrablock terpolymers (number-average molar mass, M_n = 27 kg mol^{-1}; molar mass dispersity, $Đ$ = 1.09; volume fractions, f_{PS} = 0.40, f_{PI} = 0.39, f_{PLA} = 0.21; f_{PS} divided roughly equally between the first and third blocks) were prepared by spin coating onto a hexamethyldisilazane (HMDS) treated Si wafers from dilute chlorobenzene solutions. The HMDS treatment was done to improve compatibility between the substrate surface (E_{surf}^{Si} = 61 mJ/m^2; $E_{surf}^{HMDS\text{-}Si}$ = 43 mJ/m^2)[61] and the polymer blocks (E_{surf}^{PI} = 32 mJ/m^2; $E_{surf}^{PS} \approx E_{surf}^{PLA} \approx$ 40 mJ/m^2).[26] An AFM image representative of an "as-spun" film of PS−PI−PS−PLA is shown in Figure 1. For all films, initial film thickness (T_0) after spin coating was measured using ellipsometry. Images of the film surface were acquired using tapping mode atomic force microscopy (AFM) and the expected contrast was apparent between the soft PI domains (darker) and the harder PS and PLA domains (lighter). The as-spun films display perpendicular and parallel cylindrical light domains in a dark matrix, consistent with PS/PLA cylinders in a PI matrix. The observed microphase-separated structure is consistent with a nonequilibrium mixed cylindrical orientation because of fast evaporation of solvent during spin coating as expected.

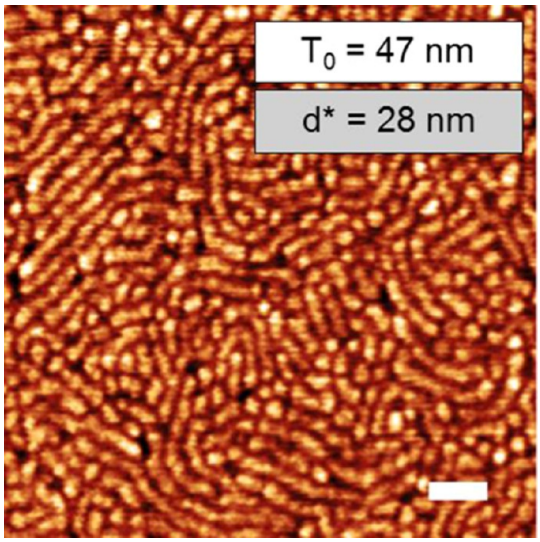

Figure 1. A representative AFM image of a thin film of PS−PI−PS−PLA as-spun from chlorobenzene onto an HMDS modified Si substrate. T_0 is the thickness as measured by ellipsometry and d* is the principal domain spacing as calculated from a fast Fourier transform (FFT) image analysis. Scale bar = 100 nm.

Solvent annealing of the thin films was carried out in a home-built chamber (Figure S1) to facilitate a controlled solvent environment. After SVA with chloroform, toluene, or THF, parallel cylinder orientation was consistently observed in the PS−PI−PS−PLA films. Representative AFM images after solvent annealing for 5 min are shown in Figure 2. The spacing between parallel cylinders from the AFM images, d^*, is similar to the bulk cylinder-to-cylinder spacing determined by SAXS (33.0 nm).[32] Islands and holes were observed across film surfaces when T_0 was not commensurate with the domain spacing. Islands contained parallel oriented cylinders, as did films annealed for a full 20 min (Figure S2).

Addition of a selective cosolvent has been previously reported to trigger a switch from parallel to perpendicular cylinders.[45,50] Therefore, to access perpendicular cylinder orientation, PS−PI−PS−PLA films were also solvent annealed in mixed solvent vapor containing THF and acetone and imaged with AFM (Figure 3). Perpendicular cylinders were observed with 30% acetone and 50% acetone by volume after 5 min of SVA. The 30% acetone annealed films contained more hexagonally ordered domains than the 50% acetone annealed films that had more grain defects and contained a mixture of perpendicular and short parallel cylinders at the film surface. Films annealed in 70% acetone contained either an interpenetrating network (Figure 3c) or a mixture of parallel and perpendicular cylinders (Figure 3d) depending on the film thickness. Brighter domains were observed in some of the films annealed with 70% acetone as the high acetone content disfavored the PI wetting layer that covers the surface of most of the films in this work (Figures 3c and S3c). Extended SVA for 20 min resulted in parallel cylinder orientation for the 30% and 50% acetone solvent mixtures (Figure S3).

SEM was used to image the surface morphology of the solvent annealed PS−PI−PS−PLA thin films after basic hydrolysis to remove PLA (Figure 3e−h). Hexagonally packed nanopores were observed post-etching for the films annealed in the 30% and 50% acetone solvent systems, whereas a porous network (at $T_0 \approx 1.2\ L_0$) or pores in a perforated lamellar

DOI: 10.1021/acsami.5b08856
ACS Appl. Mater. Interfaces 2015, 7, 27331−27339

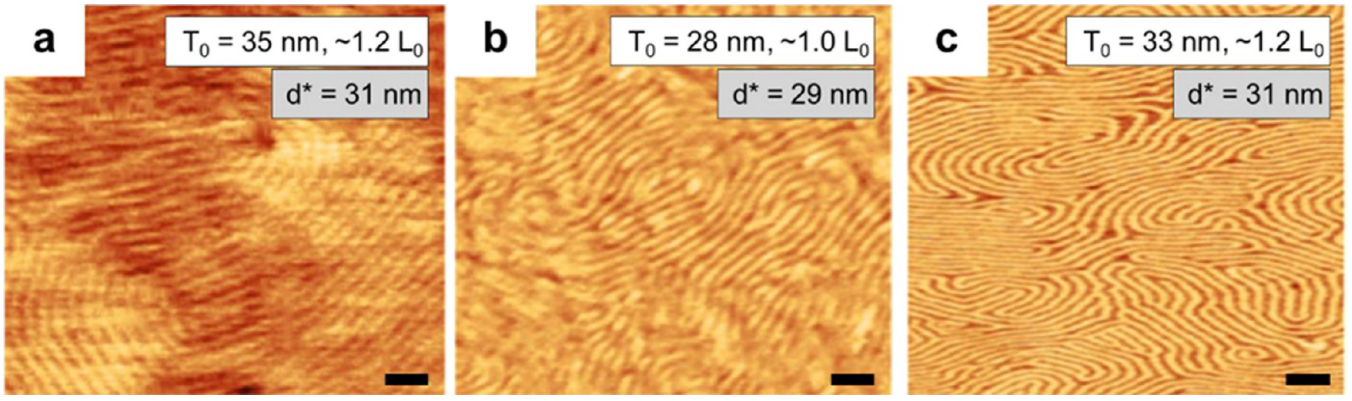

Figure 2. AFM images of PS−PI−PS−PLA thin films after solvent vapor annealing (SVA) for 5 min with chloroform (a), toluene (b), and THF (c). Listed principal domain spacings, *d**, represent the lateral distance between parallel domains at the surface. Scale bars = 100 nm.

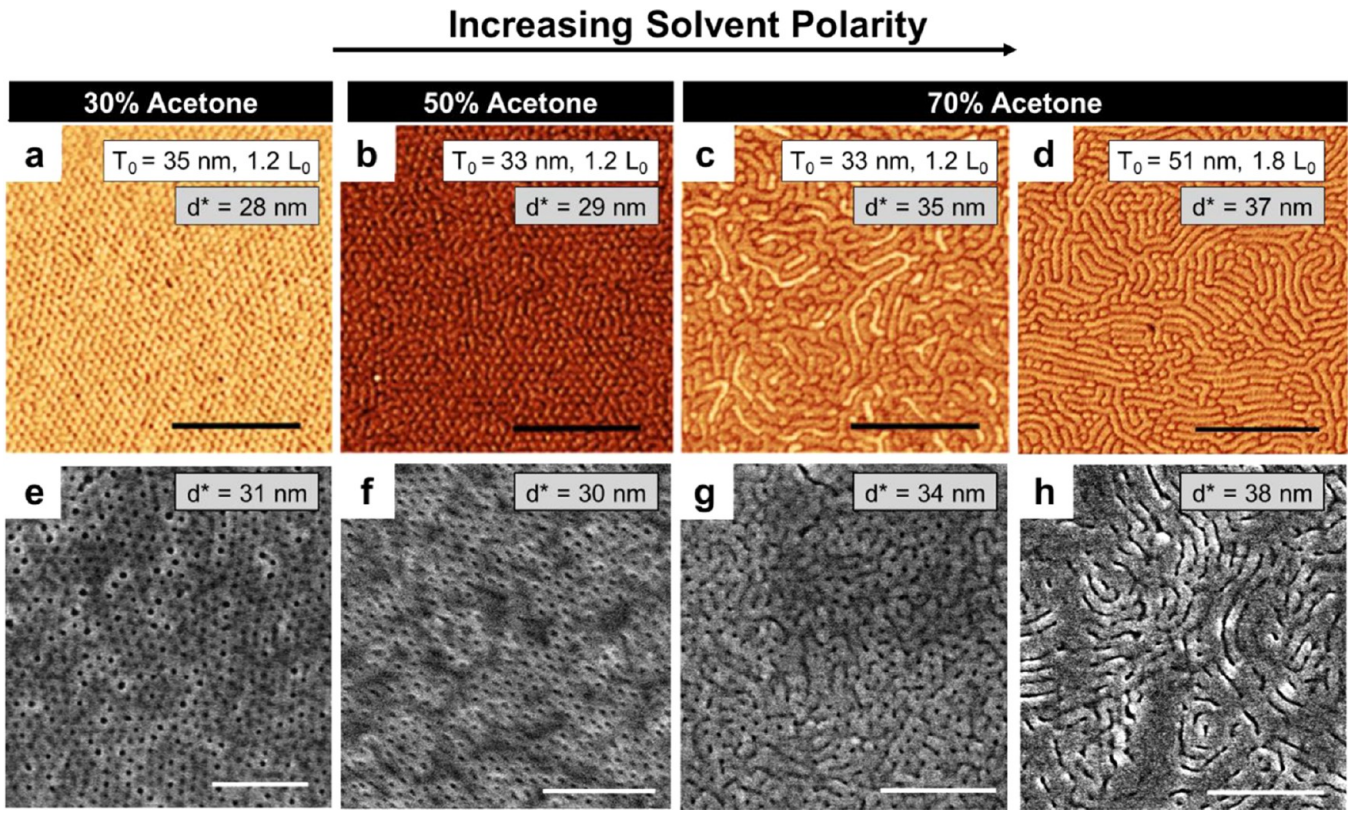

Figure 3. AFM images of PS−PI−PS−PLA films after SVA in THF/acetone mixtures with 30% acetone (a), 50% acetone (b), and 70% acetone (c and d) by volume. SEM images of the annealed films after base etching of PLA are shown below the corresponding AFM images (e−h). Black scale bars = 500 nm; white scale bars = 300 nm.

morphology ($T_0 \approx 1.8\ L_0$) were observed post-etching for the films annealed in the 70% acetone solvent system. The SEM images confirmed the assigned morphologies of the thin films pre-etching.

While SVA with more PS/PI selective solvents (chloroform, toluene, and THF) consistently resulted in parallel cylinder orientation, increasing the polarity of the annealing solvent with ~30% acetone lead to the formation of perpendicular PLA cylinders at shorter time periods. This phenomenon was optimized when the concentration of acetone in the solvent nearly matched the concentration of PLA in the block polymer (~30−50%), and the best solvent atmosphere for achieving well-ordered perpendicular cylinder domains was the 30% acetone and 70% THF mixture by volume. Increasing the acetone concentration above 50% led to a change in the morphology to a network-like structure. Compared to the other solvents used, the 70/30 THF/acetone (v/v) solvent system is the most neutral for PI, PS, and PLA, as it splits the difference between the solubility parameters of PLA and PI.[62] The change to parallel orientation of cylinders at longer annealing times, even with the optimal solvent system, suggests that the cylinder orientation is time dependent. This dependency may be due to changes in the swollen film thickness over time during SVA, which could lead to a different swollen film structure.[28]

SAXS data from solutions of PS−PI−PS−PLA in the 70/30 THF/acetone (v/v) solvent system were investigated to gain insight into the swollen film morphology prior to drying. Three samples were made containing 25%, 50%, and 75% polymer (by

DOI: 10.1021/acsami.5b08856
ACS Appl. Mater. Interfaces 2015, 7, 27331−27339

mass). No scattering was observed for the 25% polymer mixture. Figure 4 shows scattering consistent with a disordered

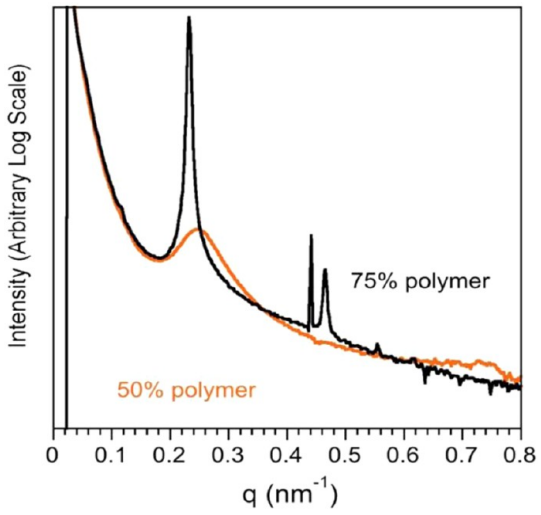

Figure 4. SAXS of PS−PI−PS−PLA swollen with the 70/30 THF/acetone (v/v) solvent system. SAXS was measured for mixtures containing 25%, 50%, and 75% polymer (by mass). Scattering from the 75% polymer mixture, black curve, indicates either cylinders or lamellae while scattering from 50% mixture shows a disordered structure. No data from the 25% mixture is displayed because the sample did not scatter. The sharp peak at ~0.44 nm^{-1} is an artifact in the scattering data.

structure at 50% polymer and consistent with either cylinders or lamellae at 75% polymer. A principal domain spacing of 27 nm (q^* = 0.23 nm^{-1}) was calculated for the 75% polymer mixture. Film thicknesses and scattering profiles were not measured during swelling of polymer thin films.

Examination of the SAXS data can provide some insight into why this specific solvent system (70/30 THF/acetone (v/v)) was so effective in producing films with perpendicular PLA cylinders. In the SAXS results for PS−PI−PS−PLA in 70/30 THF/acetone (v/v), a slight decrease in the domain spacing was observed (28.6 nm bulk vs 27 nm 75% polymer solution), suggesting that there is a lower degree of segregation between blocks in the presence of the solvent. The SAXS data indicate that while there is some order at 50% polymer, the mixture is near the order−disorder transition (ODT). A sample that in the swollen state is just on the ordered side of the ODT is in the ideal window for achieving high degrees of long-range order when dried.[28] Together, the SAXS and AFM results show that the 70/30 THF/acetone (v/v) solvent system effectively mediates the interfacial tensions between the blocks and thereby favor the formation of perpendicular cylinders.

Film thickness also plays an important role in the resultant thin film morphology. For film thicknesses between 28 and 30 nm ($T_0 \approx L_0$), mostly perpendicular cylinder orientation was observed with 30% acetone by volume. As the film thickness was increased from 28 to 60 nm (1−2 L_0), films displayed progressively more evidence of parallel orientation of cylinders across the film surface (Figure 5). Films thicker than 60 nm (~2 L_0) contained only parallel cylinder orientation. Parallel cylinder orientation in these thicker films was observed in films annealed for 5 min (Figure 5c) and 20 min (Figure S3a).

Generally, as copolymer film thickness increases, perpendicular orientation is more difficult to obtain.[56] Even with neutral interfaces (substrate and surface/air) and solvents for the polymer blocks, parallel orientation may occur. Theory and simulations have predicted that perpendicular arrays of cylinders should be obtainable at all thicknesses when neutral interfaces are used,[63] but experimental verification is lacking. Furthermore, copolymers with a large difference in surface energy can be difficult to orient even with neutral substrate and film surface interfaces.[56]

Because very specific film thicknesses and solvent systems were required to access perpendicular cylinder orientation of the tetrablock terpolymers thin film, a change in approach was required to bias the system toward the desired perpendicular morphology. Ideally, a method with greater tolerance for variation in film thickness and SVA conditions could be applied. To that end, PLA homopolymer (M_n = 10 kg mol^{-1}) was synthesized and added to the PS−PI−PS−PLA block polymer. Polymer films were prepared from spin coating dilute solutions of 95/5 or 90/10 PS−PI−PS−PLA/PLA (w/w) polymer blends in chlorobenzene onto HMDS modified Si wafers (at 1500, 2000, and 3000 rpm). This homopolymer was specifically targeted due to the $M_{n,homo\ PLA}/M_{n,PLA\ block}$ molar mass ratio of 1.4 (near the ideal 1.5 ratio[56]).

Spin coated films containing the 95/5 PS−PI−PS−PLA/PLA (w/w) polymer blend were solvent annealed for 5 min in 70/30 THF/acetone (v/v) (the preferred system for the PS−PI−PS−PLA tetrablock). Surface AFM images of solvent annealed PS−PI−PS−PLA/PLA films are shown in Figure 6.

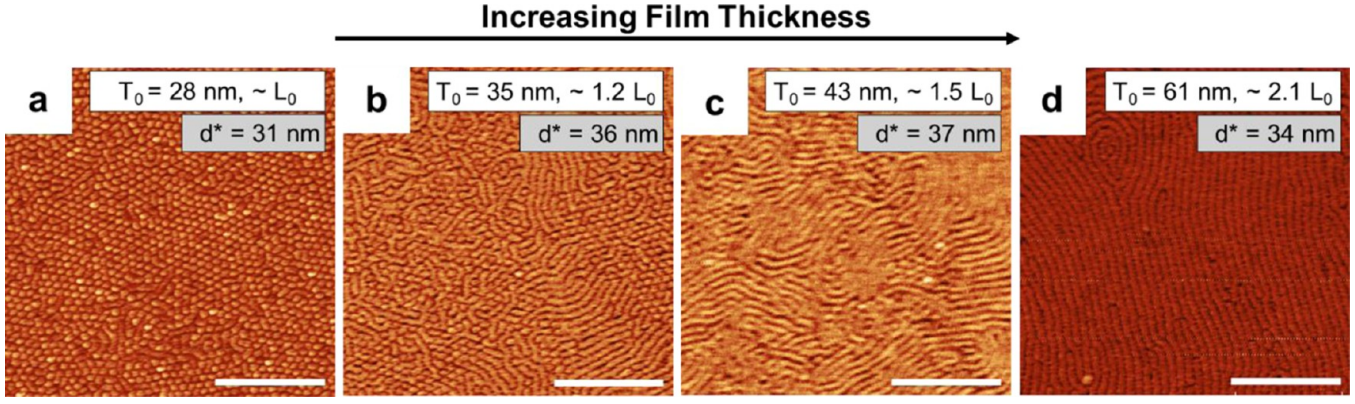

Figure 5. AFM images of PS−PI−PS−PLA films after 5 min of SVA in 70/30 THF/acetone (v/v). Film thickness increases from left to right, 28 (a) to 35 (b) to 43 (c) to 61 (d) nm, respectively. Scale bars =500 nm.

DOI: 10.1021/acsami.5b08856
ACS Appl. Mater. Interfaces 2015, 7, 27331−27339

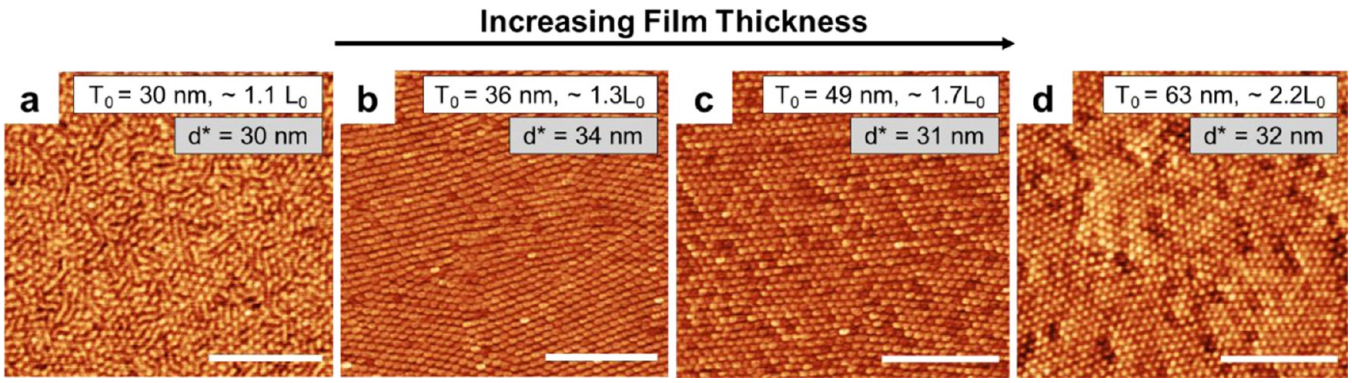

Figure 6. AFM images of 95/5 PS–PI–PS–PLA/PLA (w/w) polymer blend films after SVA in 70/30 THF/acetone (v/v). Film thickness increases from left to right: 28 (a) to 35 (b) to 43 (c) to 61 (d) nm, respectively. Scale bars = 500 nm.

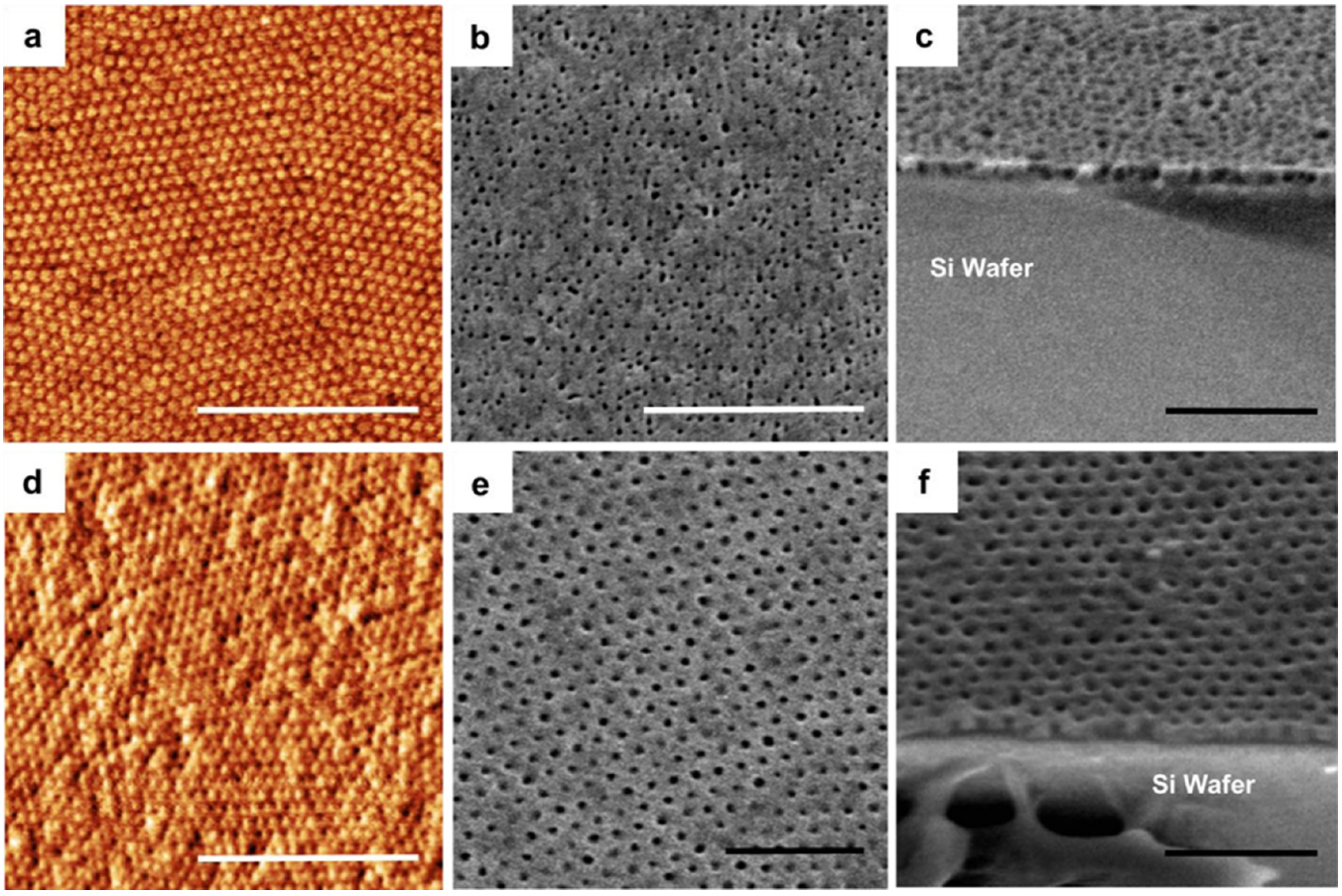

Figure 7. Images of a 95/5 PS–PI–PS–PLA/PLA (w/w) polymer blend film after spin coating from a 2 wt % solution at 3000 rpm and SVA in 70/30 THF/acetone (v/v) for 5 min (thickness = 48 nm). Post-SVA (d^* = 32 nm) (a), after basic etching (b and c), after RIE without basic etching (d), after RIE and basic etching (e and f). Cross-sectional images show perpendicular cylinder orientation (c and f). White scale bars = 500 nm; black scale bars = 200 nm.

Remarkably, after 2 or 5 min of SVA, PS–PI–PS–PLA/PLA films exhibit a perpendicular orientation at all thicknesses between 30 and 100 nm (Figures 6 and S4). Even after 10 min of SVA, only thicknesses >60 nm result in parallel orientation (Figure S4). The most well-ordered perpendicular arrays, with ordered grains as wide as 2 or 3 square microns across, resulted from 5 min of SVA in 70/30 THF/acetone (v/v) (Figure S5). Changing the ratio of tetrablock to homopolymer to 90/10 resulted in well-ordered films, though there were more defects and d^* increased from about 31 nm to about 37 nm (Figure S6). On the basis of the successful perpendicular orientation of domains using PLA homopolymer, PS–PI–PS was added to the tetrablock polymer to test for a bias in alignment based on the presence of the triblock. The 85/15 PS–PI–PS–PLA (w/w) polymer blend films did not display dependable long-range order, though a predominantly perpendicular cylindrical morphology was observed (Figure S7). The added triblock polymer would have to span both PS and PI domains and the effect on cylinder orientation was not as reliable as the addition of homopolymer that is relegated to only one domain.

The addition of 5 wt % PLA homopolymer allowed thickness independent perpendicular orientation of PLA cylinders in

DOI: 10.1021/acsami.5b08856
ACS Appl. Mater. Interfaces 2015, 7, 27331–27339

films up to 100 nm thick and improved lateral ordering of hexagonally packed grains. In fact, films from 95/5 PS–PI–PS–PLA/PLA (w/w) polymer blends were solvent annealed in the 70/30 THF/acetone (v/v) atmosphere at multiple times on multiple days (Figure S8) and after 5 min of SVA all of the films contained perpendicularly oriented cylinders regardless of film thickness, confirming the reproducibility of this procedure.

Again, SEM was used to image the surface morphology of the solvent annealed thin films after basic hydrolysis was used to remove PLA (Figure 7). Initially, only about half of the expected surface pore volume was evident by SEM due to an unetchable wetting layer (Figure 7b). AFM can be misleading as to whether all the PLA cylinders reach the surface of the film; because the image contrast is based on contrast in the moduli of the phases, such that a film with a thin wetting layer of PI may look very similar to one without. To remove the wetting layer, an oxygen (O_2) plasma reactive ion etch (RIE) step was used. A representative film surface after RIE is shown in Figure 7d. Following the RIE step, basic hydrolysis was completed to remove the newly exposed PLA domains. SEM images show well-ordered hexagonally packed nanopores 15 nm in diameter after RIE followed by basic hydrolysis (Figures 7e, f and S9). The structure is apparent across the entire film surface after RIE and basic hydrolysis (Figure 8).

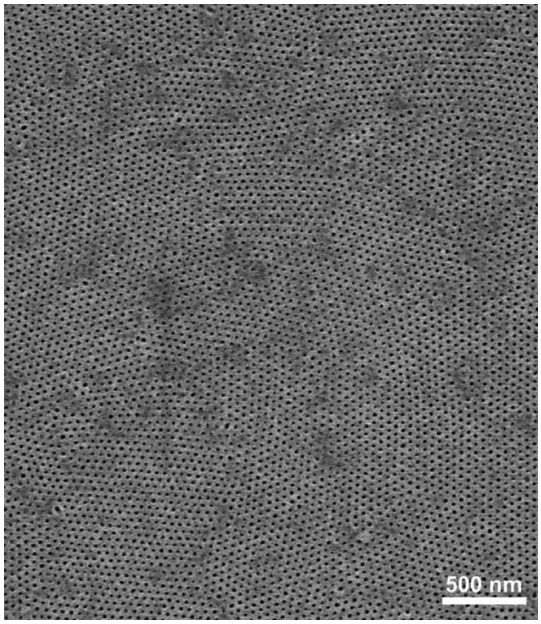

Figure 8. Large area SEM image of 90 nm thick 95/5 PS–PI–PS–PLA/PLA (w/w) polymer blend film after SVA, RIE, and PLA removal. Scale bar = 500 nm.

SEM cross-sectional analysis and images of the bottom surface of the film after RIE and basic hydrolysis of PLA provide evidence that the pores span the film thickness and reach the underlying substrate for film thicknesses up to 100 nm (Figures 7c, f and 9). The PLA etched polymer film and Si wafer were separated by coating the top of the polymer film in a thin layer of room temperature setting epoxy and then immersing the epoxy coated film in a liquid N_2 for at least 1 min. Using this method, the epoxy/block polymer film portion separated from the Si wafer naturally or with a slight tap of the wafer on a hard surface. The image shown in Figure 9b presents pores that were formed by etching from the surface of the film

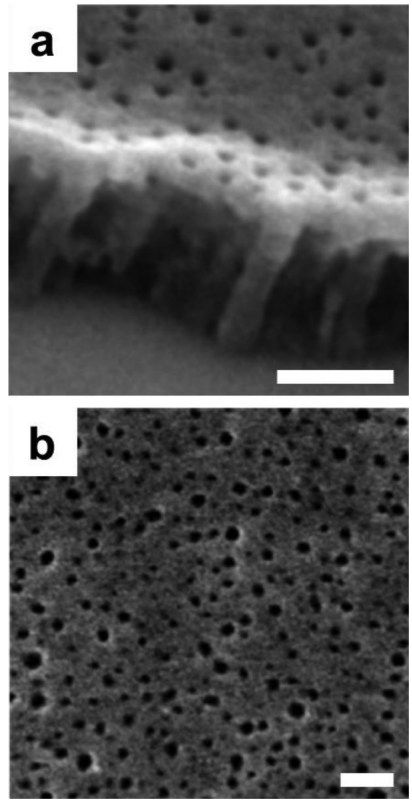

Figure 9. Cross-sectional SEM image of a porous 95/5 PS–PI–PS–PLA/PLA (w/w) polymer blend film showing vertical cylindrical pores (T_0 = 99 nm) (a). Representative SEM image of the bottom surface of an etched 95/5 PS–PI–PS–PLA/PLA (w/w) polymer blend film viewed after being removed from the underlying Si wafer (T_0 = 90 nm) (b). Scale bars = 100 nm.

before the film was transferred from Si wafer to epoxy. The bottom surface contains a mixture of larger domains and smaller dots much like the surface of the film before RIE. This structure could similarly be due to a wetting layer at the substrate interface or could result from incomplete removal of PLA homopolymer.

CONCLUSIONS

Solvent vapor annealing and homopolymer blending techniques were used to influence the microstructure of PS–PI–PS–PLA tetrablock terpolymer thin films. A mixed solvent system containing 70% THF and 30% acetone by volume was the most effective solvent system for achieving perpendicular orientation of PLA domains for the PS–PI–PS–PLA thin films, but only for films less than $T_0 \approx 1.4\ L_0$. Annealing in less polar solvents consistently resulted in parallel cylinder orientation. Addition of 5 wt % PLA homopolymer into the film led to perpendicular cylinder orientation in films regardless of film thickness for films annealed in 70/30 THF/acetone (v/v). Well-ordered hexagonally packed 15 nm pores were generated after RIE and basic hydrolysis of PLA. Vertical pores spanning the etched films were observed by SEM, confirming that perpendicular orientation was developed through the films' entire thicknesses. These results demonstrate that despite the complexity inherent in this tetrablock polymer, highly ordered nanoporous PS–PI–PS films could be obtained in a short amount of time by appropriately tuning SVA conditions and homopolymer blending. The work presented here promises accessibility of

DOI: 10.1021/acsami.5b08856
ACS Appl. Mater. Interfaces 2015, 7, 27331–27339

well-ordered nanoporous films from complex multiblock polymers for applications such as robust nanoporous filtration membranes.

■ ASSOCIATED CONTENT

Supporting Information

The Supporting Information is available free of charge on the ACS Publications website at DOI: 10.1021/acsami.5b08856.

Diagram of solvent annealing chamber and additional AFM and SEM images of PS−PI−PS−PLA polymer and PS−PI−PS−PLA/PLA polymer blend thin films (PDF)

■ AUTHOR INFORMATION

Corresponding Author

*E-mail: hillmyer@umn.edu.

Author Contributions

§These authors contributed equally to this work, share first authorship, and are listed alphabetically.

Notes

The authors declare no competing financial interest.

■ ACKNOWLEDGMENTS

This work was supported by the National Science Foundation (DMR-1006370 and DMR-1333669) and the Pall Corporation. Parts of this work were carried out in the Characterization Facility, University of Minnesota, which receives partial support from NSF through the MRSEC program. SAXS data were obtained at the DuPont−Northwestern−Dow Collaborative Access Team (DND-CAT) located at Sector 5 of the Advanced Photon Source, a U.S. Department of Energy (DOE) Office of Science user facility operated for the DOE Office of Science by Argonne National Laboratory under Contract No. DE-AC02-06CH11357.

■ REFERENCES

(1) Fasolka, M. J.; Mayes, A. M. Block Copolymer Thin Films: Physics and Applications. *Annu. Rev. Mater. Res.* **2001**, *31*, 323−355.

(2) Hamley, I. W. Nanostructure Fabrication Using Block Copolymers. *Nanotechnology* **2003**, *24*, R39−R54.

(3) Segalman, R. A. Patterning with Block Copolymer Thin Films. *Mater. Sci. Eng., R* **2005**, *48*, 191−226.

(4) Darling, S. B. Directing the Self-Assembly of Block Copolymers. *Prog. Polym. Sci.* **2007**, *32*, 1152−1204.

(5) Tseng, Y.-C.; Darling, S. B. Block Copolymer Nanostructures for Technology. *Polymers* **2010**, *2*, 470−489.

(6) Luo, M.; Epps, T. H., III. Directed Block Copolymer Thin Film Self-Assembly: Emerging Trends in Nanopattern Fabrication. *Macromolecules* **2013**, *46*, 7567−7579.

(7) Park, M.; Harrison, C.; Chaikin, P. M.; Register, R. A.; Adamson, D. H. Block Copolymer Lithography: Periodic Arrays of ~ 10^{11} Holes in 1 Square Centimeter. *Science* **1997**, *276*, 1401−1404.

(8) Stoykovich, M. P.; Nealey, P. F. Block Copolymers and Conventional Lithography. *Mater. Today* **2006**, *9*, 20−29.

(9) Ruiz, R.; Kang, H.; Detcheverry, F. A.; Dobisz, E.; Kercher, D. S.; Albrecht, T. R.; de Pablo, J. J.; Nealey, P. F. Density Multiplication and Improved Lithography by Directed Block Copolymer Assembly. *Science* **2008**, *321*, 936−939.

(10) Bates, C.; Maher, M. J.; Janes, D. W.; Ellison, C. J.; Willson, C. G. Block Copolymer Lithography. *Macromolecules* **2014**, *47*, 2−12.

(11) Yang, S. Y.; Ryu, I.; Kim, H. Y.; Kim, J. K.; Jang, S. K.; Russell, T. P. Nanoporous Membranes with Ultrahigh Selectivity and Flux for the Filtration of Viruses. *Adv. Mater.* **2006**, *18*, 709−712.

(12) Peinemann, K.-V.; Abetz, V.; Simon, P. F. W. Asymmetric Superstructure Formed in a Block Copolymer via Phase Separation. *Nat. Mater.* **2007**, *6*, 992−996.

(13) Sperschneider, A.; Scacher, F.; Gawenda, M.; Tsarkova, L.; Muller, A. H. E.; Ulbricht, M.; Krausch, G.; Kohler, J. Towards Nanoporous Membranes Based on ABC Triblock Terpolymers. *Small* **2007**, *3*, 1056−1063.

(14) Phillip, W. A.; O'Neill, B.; Rodwogin, M.; Hillmyer, M. A.; Cussler, E. L. Self-Assembled Block Copolymer Thin Films as Water Filtration Membranes. *ACS Appl. Mater. Interfaces* **2010**, *2*, 847−853.

(15) Yang, S. Y.; Yang, J.-A.; Kim, E.-S.; Jeon, G.; Oh, E. J.; Choi, K. Y.; Hahn, S. K.; Kim, J. K. Single-File Diffusion of Protein Drugs through Cylindrical Nanochannels. *ACS Nano* **2010**, *4*, 3817−3822.

(16) Simon, P. F. W.; Ulrich, R.; Spiess, H. W.; Wiesner, U. Block Copolymer-Ceramic Hybrid Materials from Organically Modified Ceramic Precursors. *Chem. Mater.* **2001**, *13*, 3464−3486.

(17) Fink, Y.; Urbas, A. M.; Bawendi, M. G.; Joannopoulos, J. D.; Thomas, E. L. Block Copolymers as Photonic Bandgap Materials. *J. Lightwave Technol.* **1999**, *17*, 1963−1969.

(18) Black, C. T.; Guarini, K. W.; Milkove, K. R.; Baker, S. M.; Russell, T. P.; Tuominen, M. T. Integration of Self-Assembled Diblock Copolymers for Semiconductor Capacitor Fabrication. *Appl. Phys. Lett.* **2001**, *79*, 409−411.

(19) Black, C. T.; Ruiz, R.; Breyta, G.; Cheng, J. Y.; Colburn, M. E.; Guarini, K. W.; Kim, H.-C.; Zhang, Y. Polymer Self-Assembly in Semiconductor Microelectronics. *IBM J. Res. Dev.* **2007**, *51*, 605−633.

(20) Xia, G.; Wang, S.; Jeong, S.-J. A Universal Approach for Template-Directed Assembly of Ultrahigh Density Magnetic Nanodot Arrays. *Nanotechnology* **2010**, *21*, 485302.

(21) Park, C.; Yoon, J.; Thomas, E. L. Enabling Nanotechnology with Self-Assembled Block Copolymer Patterns. *Polymer* **2003**, *44*, 6725−6760.

(22) Hawker, C. J.; Russell, T. P. Block Copolymer Lithography: Merging "Bottom-Up" with "Top-Down" Processes. *MRS Bull.* **2005**, *30*, 952−966.

(23) Zalusky, A. S.; Olayo-Valles, R.; Wolf, J. H.; Hillmyer, M. A. Ordered Nanoporous Polymers from Polystyrene-polylactide Block Copolymers. *J. Am. Chem. Soc.* **2002**, *124*, 12761−12773.

(24) Ho, R.-M.; Tseng, W.-H.; Fan, H.-W.; Chiang, Y.-W.; Lin, C.-C.; Ko, B.-T.; Huang, B.-H. Solvent-Induced Microdomain Orientation in Polystyrene-*b*-poly(L-lactide) Diblock Copolymer Thin Films for Nanopatterning. *Polymer* **2005**, *46*, 9362−9377.

(25) Cavicchi, K. A.; Russell, T. P. Solvent Annealed Thin Films of Asymmetric Polyisoprene-polylactide Diblock Copolymers. *Macromolecules* **2007**, *40*, 1181−1186.

(26) Kubo, T.; Wang, R. F.; Olson, D. A.; Rodwogin, M.; Hillmyer, M. A.; Leighton, C. Spontaneous Alignment of Self-Assembled ABC Triblock Terpolymers for Large-Area Nanolithography. *Appl. Phys. Lett.* **2008**, *93*, 133112.

(27) Baruth, A.; Rodwogin, M. D.; Shankar, A.; Erickson, M. J.; Hillmyer, M. A.; Leighton, C. Non-Lift-Off Block Copolymer Lithography of 25 nm Magnetic Nanodot Arrays. *ACS Appl. Mater. Interfaces* **2011**, *3*, 3472−3481.

(28) Baruth, A.; Seo, M.; Lin, C. H.; Walster, K.; Shankar, A.; Hillmyer, M. A.; Leighton, C. Optimization of Long-Range Order in Solvent Vapor Annealed Poly(styrene)-*block*-poly(lactide) Thin Films for Nanolithography. *ACS Appl. Mater. Interfaces* **2014**, *6*, 13770−13781.

(29) Lee, S.; Gillard, T. M.; Bates, F. S. Fluctuations, Order, and Disorder in Short Diblock Copolymers. *AIChE J.* **2013**, *59*, 3502−3513.

(30) Cushen, J. D.; Bates, C. M.; Rausch, E. L.; Dean, L. M.; Zhou, S. X.; Willson, C. G.; Ellison, C. J. Thin Film Self-Assembly of Poly(trimethylsilylstyrene-*b*-D,L-lactide) with Sub-10 nm Domains. *Macromolecules* **2012**, *45*, 8722−8728.

(31) Querelle, S. E.; Jackson, E. A.; Cussler, E. L.; Hillmyer, M. A. Ultrafiltration Membranes with a Thin Poly(styrene)-*b*-poly(isoprene) Selective Later. *ACS Appl. Mater. Interfaces* **2013**, *5*, 5044−5050.

DOI: 10.1021/acsami.5b08856
ACS Appl. Mater. Interfaces 2015, 7, 27331−27339

(32) Jackson, E. A.; Lee, Y.; Hillmyer, M. A. ABAC Tetrablock Terpolymers for Tough Nanoporous Filtration Membranes. *Macromolecules* **2013**, *46*, 1484−1491.
(33) Bluemle, M. J.; Fleury, G.; Lodge, T. P.; Bates, F. S. The O^{52} Network by Molecular Design: CECD Tetrablock Terpolymers. *Soft Matter* **2009**, *5*, 1587−1590.
(34) Lee, S.; Bluemle, M. J.; Bates, F. S. Discovery of a Frank-Kasper σ Phase in Sphere-Forming Block Copolymer Melts. *Science* **2010**, *330*, 349−353.
(35) Bluemle, M. J.; Zhang, J.; Lodge, T. P.; Bates, F. S. Inverted Phases Induced by Chain Architecture in ABAC Tetrablock Terpolymers. *Macromolecules* **2010**, *43*, 4449−4452.
(36) Zhang, J.; Bates, F. Dodecagonal Quasicrystalline Morphology in a Poly(styrene-*b*-isoprene-*b*-styrene-*b*-ethylene oxide) Tetrablock Terpolymer. *J. Am. Chem. Soc.* **2012**, *134*, 7636−7639.
(37) Zhang, J.; Sides, S.; Bates, F. Ordering of Sphere Forming SISO Tetrablock Terpolymers on a Simple Hexagonal Lattice. *Macromolecules* **2012**, *45*, 256−265.
(38) Sinturel, C.; Vayer, M.; Morris, M.; Hillmyer, M. A. Solvent Vapor Annealing of Block Polymer Thin Films. *Macromolecules* **2013**, *46*, 5399−5419.
(39) Schäffer, E.; Thurn-Albrecht, T.; Russell, T. P.; Steiner, U. Electrically Induced Structure Formation and Pattern Transfer. *Nature* **2000**, *403*, 874−877.
(40) Bang, J.; Kim, S. H.; Drockenmuller, E.; Misner, M. J.; Russell, T. P.; Hawker, C. J. Defect-Free Nanoporous Thin Films from ABC Triblock Copolymers. *J. Am. Chem. Soc.* **2006**, *128*, 7622−7629.
(41) Elbs, H.; Fukunaga, K.; Stadler, R.; Sauer, G.; Magerle, R.; Krausch, G. Microdomain Morphology of Thin ABC Triblock Copolymer Films. *Macromolecules* **1999**, *32*, 1204−1211.
(42) Gupta, M. C.; Deshmukh, V. G. Thermal Oxidative Degradation of Poly-lactic Acid. *Colloid Polym. Sci.* **1982**, *260*, 514−517.
(43) Garlotta, D. A Literature Review of Poly(lactic acid). *J. Polym. Environ.* **2001**, *9*, 63−84.
(44) She, M.-S.; Lo, T.-Y.; Ho, R.-M. Long-Range Ordering of Block Copolymer Cylinders Driven by Combining Thermal Annealing and Substrate Functionalization. *ACS Nano* **2013**, *7*, 2000−2011.
(45) Albert, J. N. L.; Bogart, T. D.; Lewis, R. L.; Beers, K. L.; Fasolka, M. J.; Hutchinson, J. B.; Vogt, B. D.; Epps, T. H., III. Gradient Solvent Vapor Annealing of Block Copolymer Thin Films Using a Microfluidic Mixing Device. *Nano Lett.* **2011**, *11*, 1351−1357.
(46) Bang, J.; Kim, B. J.; Stein, G. E.; Russell, T. P.; Li, X.; Wang, J.; Kramer, E. J.; Hawker, C. J. Effect of Humidity on the Ordering of PEO-Based Copolymer Thin Films. *Macromolecules* **2007**, *40*, 7019−7025.
(47) Jung, Y. S.; Ross, C. A. Solvent-Vapor-Induced Tunability of Self-Assembled Block Copolymer Patterns. *Adv. Mater.* **2009**, *21*, 2540−2545.
(48) O'Driscoll, S.; Demirel, G.; Farrell, R. A.; Fitzgerald, T. G.; O'Mahony, C.; Holmes, J. D.; Morris, M. A. The Morphology and Structure of PS-*b*-P4VP Block Copolymer Films by Solvent Annealing: Effect of the Solvent Parameter. *Polym. Adv. Technol.* **2011**, *22*, 915−923.
(49) Lee, D. H.; Park, S.; Gu, W.; Russell, T. P. Highly Ordered Nanoporous Template from Triblock Copolymer. *ACS Nano* **2011**, *5*, 1207−1214.
(50) Gotrik, K. W.; Hannon, A. F.; Son, J. G.; Keller, B.; Alexander-Katz, A.; Ross, C. A. Morphology Control in Block Copolymer Films Using Mixed Solvent Vapors. *ACS Nano* **2012**, *6*, 8052−8059.
(51) Chavis, M. A.; Smilgies, D.-M.; Wiesner, U. B.; Ober, C. K. Widely Tunable Morphologies in Block Copolymer Thin Films through Solvent Vapor Annealing Using Mixtures of Selective Solvents. *Adv. Funct. Mater.* **2015**, *25*, 3057−3065.
(52) Seppala, J. E.; Lewis, R. L., III; Epps, T. H., III. Spatial and Orientation Control of Cylindrical Nanostructures in ABA Triblock Copolymer Thin Films by Raster Solvent Vapor Annealing. *ACS Nano* **2012**, *6*, 9855−9862.
(53) Gotrik, K. W.; Ross, C. A. Solvothermal Annealing of Block Copolymer Thin Films. *Nano Lett.* **2013**, *13*, 5117−5122.
(54) Qiang, Z.; Zhang, L.; Stein, G. E.; Cavicchi, K. A.; Vogt, B. D. Unidirectional Alignment of Block Copolymer Films Induced by Expansion of a Permeable Elastomer during Solvent Vapor Annealing. *Macromolecules* **2014**, *47*, 1109−1116.
(55) Luo, M.; Scott, D. M.; Epps, T. H., III. Writing Highly Ordered Macroscopic Patterns in Cylindrical Block Polymer Thin Films via Raster Solvent Vapor Annealing and Soft Shear. *ACS Macro Lett.* **2015**, *4*, 516−520.
(56) Jeong, U.; Ryu, D. Y.; Kho, D. H.; Kim, J. K.; Goldbach, J. T.; Kim, D. H.; Russell, T. P. Enhancement in the Orientation of the Microdomain in Block Copolymer Thin Films upon the Addition of Homopolymer. *Adv. Mater.* **2004**, *16*, 533−536.
(57) Kim, S. H.; Misner, M. J.; Russell, T. P. Solvent-Induced Ordering in Thin Film Diblock Copolymer/Homopolymer Mixtures. *Adv. Mater.* **2004**, *16*, 2119−2123.
(58) Mykhaylyk, T. A.; Mykhaylyk, O. O.; Collins, S.; Hamley, I. W. Ordered Structures and Phase Transitions in Mixtures of a Polystyrene/Polyisoprene Block Copolymer with the Corresponding Homopolymers in Thin Films and in Bulk. *Macromolecules* **2004**, *37*, 3369−3377.
(59) Ahn, D. U.; Sancaktar, E. Perpendicularly Aligned, Size- and Spacing-Controlled Nanocylinders by Molecular-Weight Adjustment of a Homopolymer Blended in an Asymmetric Triblock Copolymer. *Adv. Funct. Mater.* **2006**, *16*, 1950−1958.
(60) Park, D. S.; Sancaktar, E. Structural Parameters for Nanocylinder Microdomains of Polystyrene-polybutadiene-polystyrene Triblock Copolymer and its Blends with Polystyrene Homopolymer. *Curr. Nanosci.* **2012**, *8*, 244−248.
(61) Lim, S. C.; Kim, S. H.; Lee, J. H.; Kim, M. K.; Kim, D. J.; Zyung, T. Surface-Treatment Effects on Organic Thin-Film Transistors. *Synth. Met.* **2005**, *148*, 75−79.
(62) Hansen, C. M. *Hansen Solubility Parameters, A User's Handbook*; CRC Press: Boca Raton, FL, 2000.
(63) Shibayama, M.; Hasegawa, H.; Hashimoto, T.; Kawai, H. Microdomain Structure of an ABC-Type Triblock Polymer of Polystyrene-poly[(4-vinylbenzyl)dimethylamine]-polyisoprene Cast from Solutions. *Macromolecules* **1982**, *15*, 274−280.

DOI: 10.1021/acsami.5b08856
ACS Appl. Mater. Interfaces 2015, 7, 27331−27339